



# Simulated moving bed enantioseparation of amino acids employing memory effect-constrained chromatography columns

Markus Fuereder<sup>1</sup>, Sven Panke<sup>2</sup>, Matthias Bechtold\*

Bioprocess Laboratory, ETH Zurich, Mattenstrasse 26, CH-4058 Basel, Switzerland

## ARTICLE INFO

### Article history:

Received 7 November 2011  
Received in revised form 27 February 2012  
Accepted 3 March 2012  
Available online 9 March 2012

### Keywords:

Simulated moving bed  
Perturbation method  
Teicoplanin aglycone  
Memory effect  
Countercurrent chromatography

## ABSTRACT

Teicoplanin aglycone-based chromatography columns (Chirobiotic TAG) enable amino acid enantioseparation with aqueous mobile phases, which perfectly accommodates the distinct hydrophilicity of most amino acids. Therefore, this stationary phase constitutes a promising option in particular for preparative-scale separations that require high feed concentrations for economic operation. However, detailed studies revealed a solute-related memory effect when this column is subjected to high loadings of amino acids, conditions that prevail in SMB operation. High loadings yield an activation of the column as indicated by increased retention times when comparing finite injection chromatograms obtained before and after the column had been subjected to a concentrated amino acid feed. This effect can be slowly reversed by flushing the column with solvent devoid of amino acid. Obviously, the activation of the stationary phase needs to be accounted for in the determination of adsorption isotherms that are used for SMB design. In this work we introduce a perturbation method adapted specifically to capture the stationary phase behaviour at SMB-like conditions. The adsorption isotherms obtained from this method indeed allowed for accurate SMB design of a methionine enantioseparation as judged by the very good agreement of experimentally obtained and model-predicted purities. Furthermore, SMB operation over 3 days with constant purities (besides deviations originating from a dip in temperature) was accomplished indicating that the adsorption behaviour in the activated state is indeed time invariant and stable long-term SMB operation with these columns is principally feasible.

© 2012 Elsevier B.V. All rights reserved.

## 1. Introduction

Over the last decades simulated moving bed (SMB) chromatography has evolved into a widely applied tool for the separation of enantiomers in the fine chemical and pharmaceutical industry [1,2]. An increasing selection of chiral stationary phases becomes commercially available and a large number of racemic mixtures have been separated successfully using SMB chromatography [3]. Due to the development of efficient design tools such as triangle theory [4,5] and the advances in process modelling fuelled by the revolution in computer processing power in the 1990s [6], SMB design can be conducted in a straightforward manner based on well-parameterized adsorption isotherms.

The SMB separation of racemic amino acids, arguably the most important class of chemicals in fine chemistry [7], poses some challenges to the selection of a suitable chiral stationary phase

material since underivatized amino acids are poorly soluble in normal phase eluents [8–10] and therefore mobile phases with high water content need to be applied. In this context, macrocyclic glycopeptide stationary phases, in particular those using teicoplanin or teicoplanin aglycone as chiral selector, constitute attractive options since various amino acid enantioseparations with sufficient selectivity using a highly aqueous mobile phases were reported [11].

Previously we investigated in detail the suitability of a commercially available teicoplanin aglycone stationary phase (Chirobiotic TAG, Sigma–Aldrich) for application in SMB enantioseparation [12]. We observed that the TAG column shows a solute-related memory effect, meaning that the adsorption behaviour depends on the loading of the column in the recent past [13]. Briefly, the retention times observed in finite injections chromatograms were different when comparing experiments made before and after overloading the column with a high concentration of racemic amino acid (Fig. 1).

Such behaviour was observed for all tested amino acids and all relevant mobile phases (those with high water content) [12,13]. In the specific case of methionine the retention time shift (RTS) can be up to 25% for the later eluting enantiomer (D-methionine). Interestingly, the selectivity after overload conditions increases compared to the regenerated state indicating an activation of the column. When flushing the column with high amounts of pure mobile phase,

\* Corresponding author. Tel.: +41 61 387 32 57; fax: +41 61 387 39 93.

E-mail addresses: [markus.fuereder@bsse.ethz.ch](mailto:markus.fuereder@bsse.ethz.ch) (M. Fuereder),

[sven.panke@bsse.ethz.ch](mailto:sven.panke@bsse.ethz.ch) (S. Panke), [matthias.bechtold@bsse.ethz.ch](mailto:matthias.bechtold@bsse.ethz.ch) (M. Bechtold).

<sup>1</sup> Tel.: +41 61 387 31 62; fax: +41 61 387 39 93.

<sup>2</sup> Tel.: +41 61 387 32 09; fax: +41 61 387 39 93.

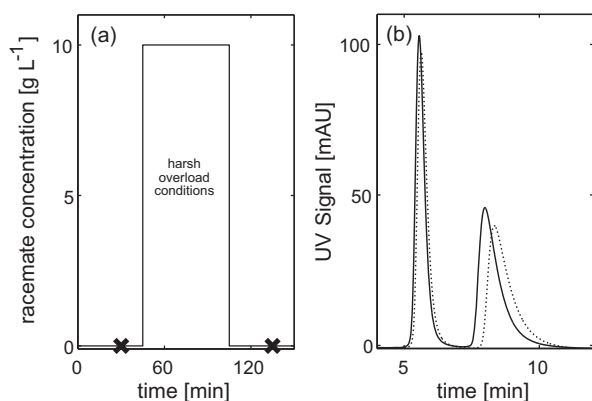


**Fig. 1.** (a) Concentration–time profile used for finite injections. The markers on the x-axis indicate the time points at which the finite injections were performed. (b) Elution profile of finite injection HPLC runs of 40  $\mu\text{g}$  racemic methionine before (solid line) and after (dashed) loaded feed treatment.

the adsorption behaviour slowly reverts to its original state, hence the effect is reversible [13]. Next, application of cyclic adsorption and desorption of large amounts of amino acid characteristic for SMB operation indicated that the adsorption behaviour assumes a steady state under such conditions and SMB operation is in principle feasible [13].

However, when designing an amino acid SMB-separation employing TAG columns, the memory effect must be taken into account since the difference between the regenerated state and the activated state is certainly not negligible (Fig. 1). Memory effect-constrained stationary phases have been occasionally reported, in particular for polysaccharide based stationary phases. In this case the change in adsorption behaviour is mediated by a component of the mobile phase and not the solute [14–16], which at least for isocratic operation allows for a straightforward SMB design. The aim of this study is (i) to identify a suitable method for isotherm parameter estimation that facilitates reliable SMB design under conditions of solute-induced memory effect and (ii) to demonstrate that stable SMB operation is feasible with such memory effect-constrained columns.

## 2. Theory

### 2.1. Perturbation method

The perturbation method constitutes a well established method for the determination of competitive isotherms, in particular for enantioseparations [6,17,18]. Briefly, it is based on the stepwise equilibration of the column with defined racemate compositions. By injection of a small pulse with concentrations that differ from the bulk concentration perturbations in the elution profile are introduced resulting in positive or negative peaks depending on the difference in concentrations of injection sample and mobile phase. In the case of a racemate, this leads to two distinct perturbation peaks in the elution profile. The retention times of the perturbation peaks can be used to derive the parameters of the underlying adsorption isotherm by obtaining the roots of Eq. (1), where  $C_1$  and  $C_2$  are the mobile phase concentrations of the enantiomers, and  $q_1$  and  $q_2$  are the concentrations of the respective enantiomers in the stationary phase.

$$\left(\frac{dC_1}{dC_2}\right)^2 + \frac{dC_1}{dC_2} \frac{(\partial q_2/\partial C_2) - (\partial q_1/\partial C_1)}{(\partial q_2/\partial C_1)} - \frac{(\partial q_1/\partial C_2)}{(\partial q_2/\partial C_1)} = 0 \quad (1)$$

The two roots of Eq. (1) are then inserted into expressions for the total derivative (Eq. (2)).

$$\frac{dq_i}{dC_i} = \sum_{j=1}^2 \frac{\partial q_i}{\partial C_j} \frac{dC_j}{dC_i} \quad i = (1, 2) \quad (2)$$

The retention times of the perturbations  $t_{R_i}$  of the respective component  $i$  can be expressed by the column hold-up time  $t_0$ , the total porosity  $\varepsilon$  and the total derivative (Eq. (3)).

$$t_{R_i} = t_0 \left(1 + \frac{1 - \varepsilon}{\varepsilon} \frac{dq_i}{dC_i}\right) \quad i = (1, 2) \quad (3)$$

Thus, with knowledge of the isotherm type the corresponding isotherm parameters can be fitted to the experimentally obtained retention times using Eqs. (1)–(3).

In this case we assumed a bi-Langmuir isotherm (Eq. (4)) with equal saturation capacities  $q_s$  for adsorption sites  $I$  and  $II$ :

$$q_i = q_{sI} \frac{b_{iI} C_i}{1 + b_{iI} C_i + b_{i2} C_2} + q_{sII} \frac{b_{iII} C_i}{1 + b_{iII} C_i + b_{i2} C_2} \quad i = (1, 2) \quad (4)$$

### 2.2. SMB

Operating points for SMB experiments were chosen using heuristics of the triangle theory, which indicates the region of complete separation as a function of the respective flow rate ratios  $m$  of zone II and III. The flow rate  $Q_j$  in zone  $j$  can then be calculated from  $m_j$ , the selected switch time  $t^*$ , the bed porosity  $\varepsilon$ , the volume of the column  $V$  and the extra column volume  $V_{Dj}$  (Eq. (5)).

$$Q_j = \frac{m_j V (1 - \varepsilon) + V \varepsilon + V_{Dj}}{t^*} \quad (j = 1, \dots, 4) \quad (5)$$

For details on the  $m_{II}$ – $m_{III}$  diagram and the triangle theory please refer to the works of Mazzotti, Morbidelli and Storti [4,19]. In order to rapidly generate the region of complete separation, a short cut method [20] was used. Single SMB runs were simulated using a more detailed SMB model described in [21]. The detailed SMB model allowed (i) the simulation of the dynamic development of concentration profiles with time, (ii) the inclusion of detailed kinetic data for each enantiomer, and (iii) the detailed column configuration in the SMB device.

## 3. Experimental

### 3.1. Chemicals

Methionine, ammonium acetate ( $\text{NH}_4\text{Ac}$ ) and all other chemicals were either purchased from Roth (Reinach, Switzerland) or Sigma–Aldrich (Buchs, Switzerland) unless stated otherwise. Acetonitrile was purchased from Chemie Brunschwig (Basel, Switzerland). All organic solvents were HPLC grade. Deionized water was obtained from a TKA–Genpure machine.

### 3.2. Columns

For analytical measurements we used a stainless steel Chirobiotic TAG column (100 mm  $\times$  4.6 mm ID) with a particle diameter of 5  $\mu\text{m}$ . The applied five preparative columns (100 mm  $\times$  10 mm ID) were equipped with 16  $\mu\text{m}$  beads. All were obtained from Sigma–Aldrich (St. Louis, USA). The preparative columns had been used to different extents before this study.

### 3.3. Analytics

All analytical measurements as well as adsorption isotherm measurements were performed at 22  $^\circ\text{C}$  on an Agilent 1100 HPLC

system with a diode array detector. A refractive index detector was employed for the detection of deuterated water for the determination of column dead volume. Analytical measurements to quantify L- and D-methionine concentrations were performed using 90/10% (v/v) 50 mM NH<sub>4</sub>Ac pH 6.0/methanol mobile phase at a flow rate of 1.5 mL min<sup>-1</sup>.

### 3.4. Perturbation measurements

The principle of adsorption isotherm determination using the perturbation method relies on the stepwise saturation of the column with known concentrations of solute. Perturbations were introduced by injecting samples of 10 μL with concentrations that slightly differed from the applied equilibrium plateau. Perturbation retention times of L- and D-methionine were recorded at 15 different concentration levels ranging from 0 to 12 g L<sup>-1</sup> racemic methionine. Different collocations of concentration levels were used in this study. “intermediate”: Collocation with intermediate plateau (given in g L<sup>-1</sup> racemic methionine): 0/8/2/8/1.6/8/1.2/8/0.8/8/0.4/8/0.2/8/0.16/8/0.12/8/0.08/8/0.04/8/0.02/8/0/8/8/8/4/8/12/8/0; “no-intermediate”: 0/2/1.6/1.2/0.8/0.4/0.2/0.16/0.12/0.08/0.04/0.02/0/8/4/12/0; “bottom-up”: 0/0.02/0.04/0.08/0.12/0.16/0.2/0.4/0.8/1.2/1.6/2/4/8/12; “top-down”: 12/8/4/2/1.6/1.2/0.8/0.4/0.2/0.16/0.12/0.08/0.04/0.02/0.

A graphical illustration and a detailed table of the applied concentration plateaus is provided as supplementary material (Fig. S1, Tables S1–S4).

Prior to each perturbation experiment the preparative column was regenerated for at least 30 min at 4 mL min<sup>-1</sup> with 50/50% (v/v) 50 mM NH<sub>4</sub>Ac/acetonitrile and then flushed with 90/10% 50 mM NH<sub>4</sub>Ac/methanol for 15 min.

### 3.5. SMB setup and experiments

The SMB-device is based on a modified ÄKTA basic system (GE Healthcare, Freiburg, Germany) and consists of two P-900 pump modules (GE Healthcare), five multiposition valves, and a UV/VIS detector. One pump module was assigned to provide the feed and eluent flow streams, the other module was used to control extract and raffinate flow rates. Each of the (in total) four pumps was connected to a multiposition valve PV-908 (GE Healthcare), while the fifth multiposition valve was employed to direct the eluent outlet from zone IV (open loop arrangement). Check valves (Ercatech, Switzerland) were placed between each pair of columns to ensure the correct direction of the flow. The column loop of the SMB was built from identical subunits, one of which is depicted in Fig. 2.

The extra-column dead volumes per section were measured and divided by the number of columns per section, resulting in a  $V_{Dj}$  of 0.1 mL [22]. The concentration of methionine in the raffinate was monitored with the UV-detector at 235 nm. Extract and raffinate purities were evaluated once steady-state conditions had been reached as judged by invariant raffinate outlet profiles. The time till steady state was further confirmed by detailed SMB simulations. The respective samples were collected for a period of two cycles and quantified by HPLC analysis. All outlet flow rates were additionally checked by collecting the streams for a timed period and weighing them in small flasks. The eluent and feed reservoir were degassed using a suction pump prior to the SMB experiments. Additionally, before entering the SMB system the feed and the eluent stream passed through an online degasser (Phenomenex, Torrance, USA). We applied a modified version of the standard UNICORN™ software (GE Healthcare) [23] for the control of pumps, valves, and the UV/VIS detector. Prior to each SMB run, the system was regenerated for at least 30 min at 4 mL min<sup>-1</sup> with 50/50% (v/v) 50 mM NH<sub>4</sub>Ac/acetonitrile. SMB runs were performed under two

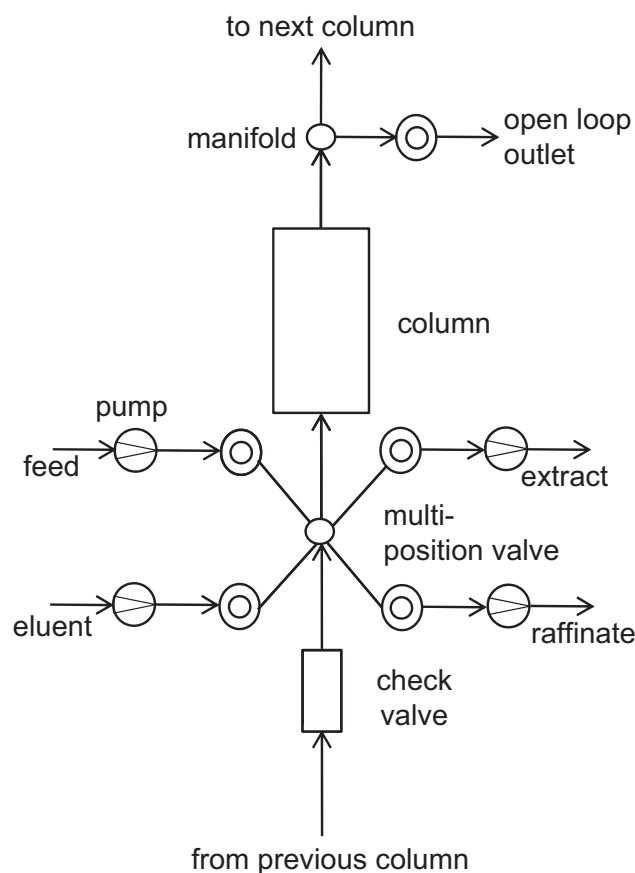


Fig. 2. SMB set-up: single column building.

distinct isocratic mobile phase regimes: 90/10% (v/v) or 75/25% (v/v) 50 mM NH<sub>4</sub>Ac pH 6.0/methanol. In each case the feed consisted of 10 g L<sup>-1</sup> racemic methionine dissolved in the respective mobile phase. All SMB runs were performed in 1–2–1–1 open loop configuration.

### 3.6. Simulation and fitting procedures

A model-based experimental analysis approach was applied in order to obtain adsorption isotherm parameters from perturbation method chromatography experiments (see Section 2). The parameterization was derived by minimizing the difference between model prediction and experimental data using an optimization algorithm. The fitting procedure was implemented in MATLAB (Mathworks, Natick, USA) and used the optimization function “fminsearch” for identifying the parameterization with the smallest residuals. The SMB models were implemented in MATLAB.

## 4. Results and discussion

The application of memory effect-constrained columns in an SMB setting, in particular when the memory effect is related to the loading of the solutes, rests on two premises: (i) the development of the adsorption behaviour assumes a steady state after a certain operation time and remains invariant for the remainder of the SMB operation and (ii) it is possible to obtain a suitable adsorption isotherm that describes this time-invariant state for SMB design. We addressed the latter point first, as this would allow us addressing the first point with a long-term SMB experiment at a meaningful operating point (such as complete separation of enantiomers).

#### 4.1. Method development

The reliable design of a SMB process is widely dependent on an accurate description of the chromatographic process in terms of thermodynamics (adsorption isotherms) and kinetics (mass transfer kinetics). Slow mass transfer yields a broadening of the concentration profile migrating through the column whose basic form is governed by the adsorption isotherm and hence can significantly influence the separation. In principle, the memory effect-induced shift in adsorption behaviour can be a result of changes in both the adsorption isotherms and mass transfer kinetics. However, there are several indications that the latter does not change by much. First of all the observed shift in retention times cannot be explained on a mechanistic level with a change of mass transfer kinetics, suggesting a change in adsorption isotherms as the main source of the memory effect. Next, the obtained finite injection profiles (Fig. 1) for the enantioseparation of methionine using memory effect-constrained Chirobiotic TAG columns after loaded feed treatment yielded very similar band broadening compared to the profiles obtained in the regenerated state indicating that mass transfer has not significantly changed. A van Deemter curve obtained from finite injections in the regenerated state of the column further indicated very efficient operation characterized by high plate numbers ( $NTP > 100$ ) for the projected flow regime (data not shown). At such high plate numbers the influence of mass transfer resistance on SMB performance is moderate and in turn SMB performance is not very sensitive to slight changes in the mass transfer characteristics [24]. Therefore, it is safe to assume that mass transfer kinetics obtained for the regenerated state provides an adequate description for the activated state of the column.

##### 4.1.1. Choice of adsorption isotherm method

A number of different methods for isotherm parameter estimation are available [17], each with distinct advantages and disadvantages. In the specific case of memory effect-constrained columns the stationary phase need to be characterized in the state that is relevant to SMB operation, hence conditions similar to SMB operation should prevail in the adsorption isotherm determination method. This effectively limits the selection to those methods based on concentration plateaus, such as the perturbation method [18,25], the inverse method on plateaus [26] and frontal analysis [6,27]. Frontal analysis typically becomes experimentally expensive when multi-component mixtures are applied as the obtained elution profiles need to be broken down into the contribution of the respective compounds, which in the case of enantiomers requires additional HPLC analysis of samples from the frontal analysis elution profile [27]. The inverse method on plateaus constitutes a hybrid method with elements from the perturbation method and the inverse method on elution profiles from simple HPLC injections [26]. Since the shape of the introduced perturbations is analyzed the information content of the experiment is improved compared to the perturbation method, hence fewer experiments are required. On the other hand the analysis of such profiles is numerically expensive. In this study, we chose to employ the perturbation method, which does not require additional HPLC analysis, allows the rapid calculation of isotherm parameters from the experimental data and was successfully applied for chiral SMB design in earlier instances [25]. Furthermore, no detector calibration is necessary and consumption of pure enantiomers is low while the increased consumption of racemate for the concentration plateaus seems acceptable due to the low cost of the racemate.

##### 4.1.2. Accounting for a memory effect in the perturbation method

In chromatographic systems that are not affected by a memory effect, the collocation of plateaus, i.e. the sequence of concentration levels in the column at which perturbations are introduced, is not

expected to have an effect on the retention times of the perturbations. In contrast, the retention times of single injections in memory effect-constrained systems were shown to be heavily dependent on the column history, i.e. on the concentration levels that preceded each respective run [13]. An SMB process is characterized by cyclic adsorption and desorption of large amounts of solute. As the loading of solute triggers the activation of columns this situation should be imitated in the adsorption determination method. Arguably, the accuracy of the estimation procedure should improve with the extent to which the conditions in the SMB can be mimicked. However, the exact SMB concentration profile inside the columns can only be estimated when operating points and conditions as well as adsorption isotherms are known, which are obviously not available at this stage of the process development. Therefore, we introduced an additional plateau of a higher concentration prior to establishing the concentration regime for the introduction of the perturbations as a rough approximation of SMB conditions. In detail, we selected an exposure of a concentration of  $8 \text{ g L}^{-1}$  of racemic methionine for 10 min for the additional plateau, which appeared reasonable in the face of potential racemic feed concentrations of  $25 \text{ g L}^{-1}$  (solubility limit) for the projected mobile phase of 90/10% (v/v) 50 mM  $\text{NH}_4\text{Ac}$  pH 6.0/methanol.

#### 4.2. Reproducibility and column heterogeneity

Before evaluating the usefulness of the proposed adsorption isotherm determination method on the basis of experimental SMB runs, the run-to-run reproducibility and column-to-column heterogeneity of the proposed method need to be investigated. The inaccuracies originating from the experimental procedure and heterogeneity of the applied columns are propagated to the SMB design and hence are sources of errors besides the potential inability of the method to adequately characterize the memory effect-constrained adsorption behaviour.

##### 4.2.1. Reproducibility

In order to investigate the robustness and run-to-run reproducibility of the presented method, triple runs were conducted under identical conditions with the same column. The relative standard deviations (RSDs) of the first eluting perturbation had an average value of 0.2% at an average retention time of 5.2 min and had a value of 0.38% for the later eluting perturbation at an average retention time of 7.0 min. The observed variability in retention times of the perturbations was much smaller compared to the shift in retention times induced by the memory effect [13]. This indicated that the adsorption behaviour under overload condition could be reproduced under controlled conditions. In addition, the experimental error of the presented method was rather low.

##### 4.2.2. Column heterogeneity

The homogeneity of the column set constitutes an important aspect for the accurate prediction of an SMB separation. Usually the thermodynamic parameters of only one column are applied for the simulation of SMB performance. Muhlbacher et al. showed that the area of complete separation decreases when column variability is increased [28,29]. This effect is especially pronounced for feed concentration regimes in which the adsorption behaviour is in the non-linear range. Because the preparative columns applied in this study had been used to different extents before the experiments reported here, we wanted to assess the variability of the thermodynamic properties of the columns. A second purpose of this comprehensive analysis was to identify a specific column that could adequately represent the behaviour of the whole multi-column system. Thus, when assessing SMB performance for other conditions the design could be based on the isotherm obtained from this representative column without the need to assess all applied

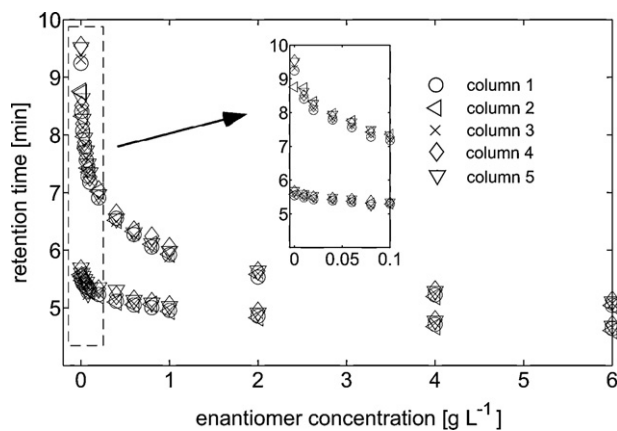


**Fig. 3.** Retention times of perturbations as a function of the methionine enantiomer concentrations for all columns 1–5 obtained from the intermediate plateau sequence. The inset shows the perturbation retention times at a concentration range from 0 to 0.1 g L<sup>-1</sup> enantiomer concentration.

columns. Therefore, we performed perturbation measurements for all columns (Fig. 3).

The average RSD of pulse retention times in between the five columns was 1.0% for the first eluting perturbation and 1.3% for the second eluting perturbation. The column-to-column variability was particularly high at low concentrations. At a concentration of 0 g L<sup>-1</sup> racemate in the mobile phase (essentially finite injection HPLC conditions) the RSD for the second peak was 3.4%, while at the highest concentration of 12 g L<sup>-1</sup> racemate, corresponding to 6 g L<sup>-1</sup> of the respective single enantiomers, the RSD was only 0.8% for both perturbations.

The average total hold up time, measured by injection of non-retained deuterated water, was 3.42 min with an RSD of 1.0%, thus giving an averaged porosity of 0.65. Very often variability in retention times is solely attributed to differences of stationary phase porosities due to column packing effects [28]. However, the results presented here show that the variability of retention times in the low concentration range cannot be explained by differences in the density of column packing. Further, we did not observe a correlation between retention times of the non-retained compound and retention times of pulse injections of methionine. This indicates that the column-to-column fluctuations arise from differences in the stationary phase itself. As mentioned the columns had been used to different extents prior to this study with some columns already heavily in use for years, which manifested itself in a slight decrease in retention times.

#### 4.3. SMB design based on the perturbation method and SMB operation

##### 4.3.1. Parameter estimation

Next, the retention times obtained by the perturbation method were used to provide a parameterized adsorption isotherm for subsequent SMB design. The first step was to examine which type of isotherm should be applied in the fitting procedure. Previous investigations on the adsorption mechanism of the methionine–teicoplanine aglycone separation system indicated at least two enantioselective adsorption sites [13]. Further, a thermodynamically (td.) non-consistent bi-Langmuir isotherm (with different saturation capacities of adsorption sites for the two enantiomers) had been successfully applied for description of HPLC elution profiles [12]. Similar isotherms were reported for various separations conducted with the closely related Chirobiotic T column [30–32], in some instances using the td. consistent form of

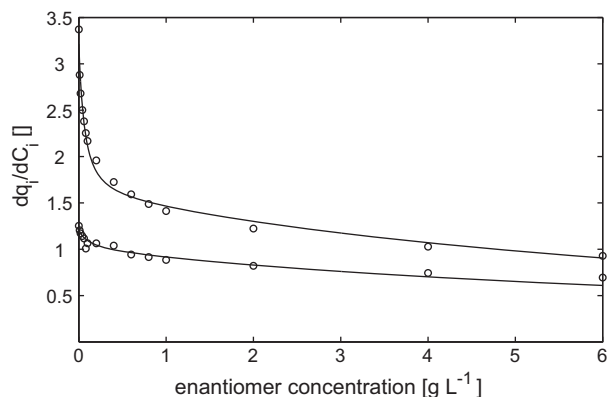


**Fig. 4.** Comparison between best-fit simulation (line) and experimental data (markers) obtained for column 5. Best-fit overlays of all other columns can be found in [supplementary material](#).

the bi-Langmuir isotherm with fewer parameters [30,33] (see Eq. (1)).

Consequently, we tested different Langmuir isotherm types, the td. consistent (6 parameters) and td. non-consistent bi-Langmuir isotherm (8 parameters) and additionally a td. consistent tri-Langmuir isotherm with two enantioselective sites (8 parameters). No significant reduction in the residual between best-fit simulation and experimental data was obtained with the higher parameterized isotherms, therefore we applied the td. consistent bi-Langmuir isotherm for analysis of the perturbation retention times obtained from the five investigated columns (Fig. 4, column 5), the remaining fitting results can be found in [supplementary section](#).

Further, an “averaged” parameterization was calculated from the averaged retention times for all 5 columns (Table 1).

The obtained parameterizations suggested a fundamentally different character of the two adsorption sites considered in the bi-Langmuir model, one with a high saturation capacity and low Langmuir constants and one with a very low saturation capacity and high Langmuir constants. The relative deviation in parameters obtained for the latter site was much higher compared to the high-saturation site, which perfectly accommodated for the larger deviations in retention times observed for small concentrations—the concentration where the second site is not overloaded and has a significant effect on the isotherm. It is worth noting that the obtained parameterizations indicate that both type of adsorption sites are enantioselective. Therefore, the applied isotherm should be treated as an empirical description because contributions of non-enantioselective interactions to the overall retention are prevalent in chiral chromatography [34].

##### 4.3.2. Comparison of experimental and simulated purities

**4.3.2.1. Methanol content of 10%.** In order to evaluate the general feasibility of the applied design strategy and to identify the most representative column for SMB design, the operation regimes indicated by the obtained isotherms were compared to the results of experimental SMB runs. Estimation of the area of complete separation in the  $m_{II}$ – $m_{III}$  plane was conducted using the short-cut method of Migliorini and Mazzotti [20] and applied to the isotherm sets of all columns. This method relies on the equilibrium theory of chromatography and thus neglects non-ideal influences such as mass transfer resistance. However, it was demonstrated that for not overly constrained systems (NTP > 100) the deviations are small and the short-cut method provides a sufficiently accurate initial estimation of the process performance [24]. In order to determine a suitable feed concentration regions of complete separation were calculated using the equilibrium theory approach [20] for different feed concentration regimes. At high concentration the

**Table 1**  
Parameters of bi-Langmuir isotherm for each column used in SMB operation.

Column	$q_{si}$ [g L <sup>-1</sup> ]	$b_{I, \text{L-Met}}$ [L g <sup>-1</sup> ]	$b_{II, \text{D-Met}}$ [L g <sup>-1</sup> ]	$q_{sl}$ [g L <sup>-1</sup> ]	$b_{II, \text{L-Met}}$ [L g <sup>-1</sup> ]	$b_{II, \text{D-Met}}$ [L g <sup>-1</sup> ]
1	32.5	0.03	0.05	0.19	1.06	7.67
2	36.4	0.03	0.04	0.34	0.56	4.14
3	35	0.03	0.04	0.21	1.1	7.29
4	32.6	0.03	0.05	0.16	1.21	9.46
5	35.3	0.03	0.05	0.23	1.01	7.18
Average 1–5	34.6	0.03	0.05	0.22	0.97	6.75

area of complete separation became so small that it was beyond the technical limits of the SMB unit to perform a robust operation. As a compromise between sufficient robustness and productivity we decided for a feed concentration of 10 g L<sup>-1</sup>.

Overlaying the position of the complete separation regions (Fig. 5) obtained from the isotherms of the different columns showed as expected some differences due to the column heterogeneity, however, no drastic outliers were observed.

This implies that the differences in parameterizations were at least not exclusively an effect of overparameterization (different sets of parameters can theoretically yield virtually the same isotherm form) but indeed are a reflection of column heterogeneity. On the basis of the regions of complete separation we chose different operating points for experimental SMB runs that supposedly covered the range from pure raffinate to complete separation and to pure extract. Of the 12 experimental runs that were performed, the 4 runs that were within each of the 5 complete separation regions (assigned to each of the 5 columns used in the experiments) showed no detectable impurities at the respective outlet ports. In general, all the experimental data indicated good agreement between experiments and short-cut simulations. However, the information that can be extracted from this short cut model is limited, e.g. no purity values at the extract and raffinate outlet ports can be obtained. With a detailed SMB model that takes into account kinetic effects, the actual column configuration, and the size and dimension of the chromatographic columns, much more profound information can be obtained. However, for the sake of simplicity we assigned the same isotherm to all columns. More precisely, we chose the parameter set that was obtained from averaged perturbation retention times of all columns used in the SMB. Next, we

included the parameters related to non-ideal conditions (solid LDF model, mass transfer coefficients  $k_{r, \text{Met}} = 1.26 \text{ s}^{-1}$ ,  $k_{d, \text{Met}} = 1.01 \text{ s}^{-1}$ , axial dispersion was calculated with the factor for axial dispersion  $A = 4.5 \times 10^{-4} \text{ m}$ , with  $D_{ax} = 0.5A u_{int}$ , with  $u_{int}$  the interstitial velocity in  $\text{m s}^{-1}$ ) that were extracted from the van Deemter plot (for details on the procedure please refer to [35]). The outlet purities obtained from the detailed SMB simulations (Table 2) showed a good agreement with the experimentally obtained values. This also supports our initial assumption that mass transfer kinetics does not significantly change under overload conditions.

**4.3.2.2. Methanol content of 25%.** One of the goals of this study was to develop a fast and reliable isotherm determination method for a number of conditions employing only one column. In order to find the most representative column we (i) compared the perturbation retention times of all columns with the averaged perturbation retention times and (ii) compared the actual thermodynamic parameters of all columns with the parameter set from averaged perturbation retention times. Both approaches yielded column 5 as the column that represented all columns to the largest extent. A comparison of the respective complete separation regions using the short-cut model is depicted in Fig. 6.

Preliminary experiments indicated that the retention times and the selectivity of the enantioseparation of racemic methionine increased with increased methanol content. In order to verify these results and to further test the validity of the presented isotherm parameter estimation method, we employed the perturbation method for eluent containing 25% methanol using the previously identified representative column (Table 3).

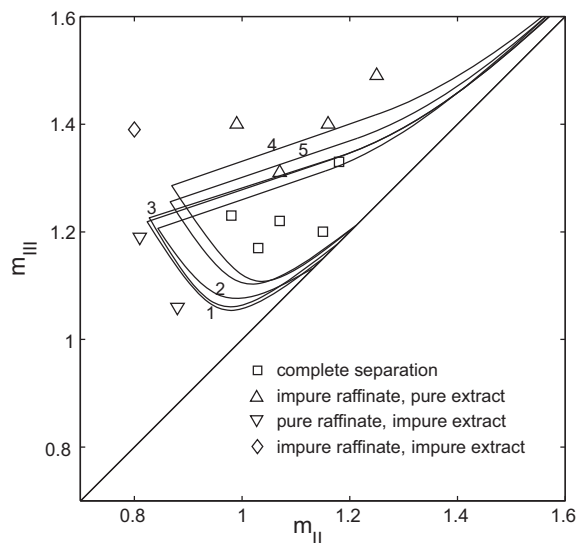


**Fig. 5.**  $m_{II}$ – $m_{III}$  diagram showing simulated complete separation regions using parameter sets for columns 1–5 compared to experimentally obtained SMB outlet purities for raffinate and extract. Details on the experimental SMB runs (markers) are provided in Table 2.

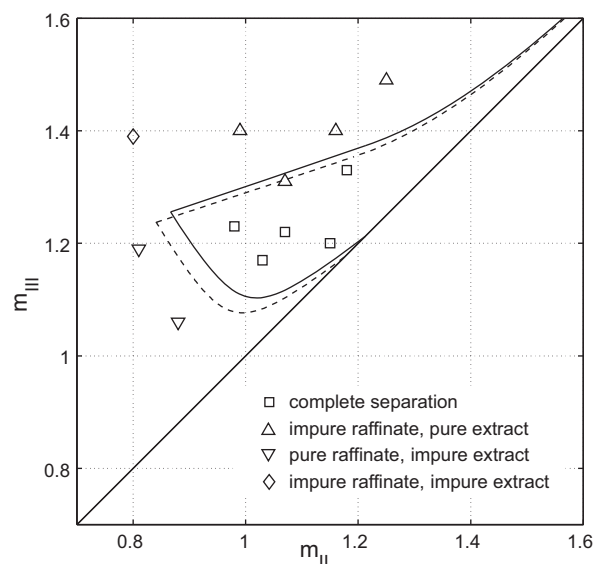


**Fig. 6.** Comparison of complete separation regions. Solid line: averaged perturbation retention times. Dashed line: perturbation retention times of column 5. Markers denote the experimental SMB runs A–L listed in Table 2.

**Table 2**

Comparison of experimentally obtained and simulated extract and raffinate purities. The detailed SMB-model was fed with isotherm parameters obtained from averaged perturbation retention times of all columns.  $E_{\text{exp}}$ : experimental extract purity [%];  $R_{\text{exp}}$ : experimental raffinate purity [%];  $E_{\text{sim}}$ : simulated extract purity [%];  $R_{\text{sim}}$ : simulated raffinate purity [%].

Run	Flow rate ratios				Purity [%]			
	$m_{\text{I}}$	$m_{\text{II}}$	$m_{\text{III}}$	$m_{\text{IV}}$	Experimental		Simulated	
					$E_{\text{exp}}$	$R_{\text{exp}}$	$E_{\text{sim}}$	$R_{\text{sim}}$
A	3.22	0.81	1.19	0.57	92	>99	98	>99
B	3.66	0.98	1.23	0.42	>99	>99	>99	>99
C	3.66	0.99	1.4	0.41	>99	76	>99	78
D	3.66	0.8	1.39	0.39	95	76	98	78
E	3.66	1.15	1.2	0.39	>99	>99	>99	99
F	3.66	1.16	1.4	0.41	>99	75	>99	82
G	3.66	1.18	1.33	0.4	>99	>99	>99	>99
H	3.66	1.07	1.31	0.41	>99	93	>99	>99
I	3.66	1.07	1.22	0.4	>99	>99	>99	99
J	3.66	1.03	1.17	0.45	95	>99	>99	>99
K	3.66	0.88	1.06	0.43	93	>99	96	99
L	3.66	1.25	1.49	0.39	>99	68	>99	68

Column configuration in the SMB: 1-2-1-1; switch time: 195 s.

**Table 3**

Parameters of bi-Langmuir isotherm of column 5 with 75/25% (v/v) 50 mM  $\text{NH}_4\text{Ac}$  pH 6.0/methanol.

Column	$q_{\text{sl}}$ [ $\text{g L}^{-1}$ ]	$b_{\text{I, Met}}$ [ $\text{L g}^{-1}$ ]	$b_{\text{II, Met}}$ [ $\text{L g}^{-1}$ ]	$q_{\text{sil}}$ [ $\text{g L}^{-1}$ ]	$b_{\text{II, Met}}$ [ $\text{L g}^{-1}$ ]	$b_{\text{II, D-Met}}$ [ $\text{L g}^{-1}$ ]
5	34.9	0.03	0.06	0.39	0.69	5.51

Indeed, when comparing the area of complete separation in the  $m_{\text{II}}-m_{\text{III}}$  diagram obtained from isotherms recorded at 10% and 25% methanol (Fig. 7), the much larger area for 25% methanol clearly indicated the potential for higher productivity and robust operation. Next, we performed two experimental SMB runs with 25% methanol content: one that was safely in the complete separation region and one that was presumably in the pure extract region.

The obtained experimental purities (Table 4) show excellent agreement with predicted purities from detailed SMB simulation supporting further the validity of the presented isotherm determination method.

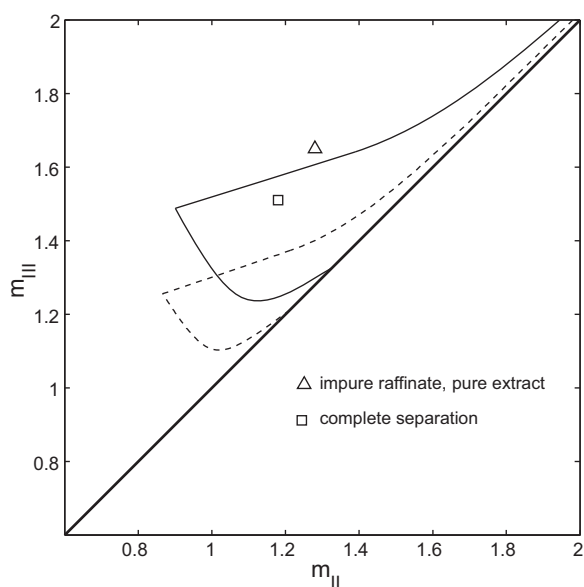


**Fig. 7.** Comparison of complete separation regions of chromatographic systems with different MeOH-contents. Full line: 90/10% (v/v) 50 mM  $\text{NH}_4\text{Ac}$  pH 6.0/methanol. Dashed line: 75/25% (v/v) 50 mM  $\text{NH}_4\text{Ac}$  pH 6.0/methanol. Markers denote the experimental SMB runs M and N listed in Table 4.

#### 4.4. Comparison of different collocation of plateaus

As discussed earlier, the collocation of concentration plateaus was selected as a rough approximation of SMB conditions. With the knowledge obtained on the adsorption isotherms and the resulting ability to estimate SMB concentration profiles in the now much better defined potential operating region, the isotherm determination method can in principle be refined to better represent SMB conditions, which then would potentially yield improved SMB operation predictions. However, at least for our purposes the observed prediction accuracy was satisfactory.

On the other hand simpler methods without intermediate plateau might yield an equally good adsorption isotherm description. In order to check whether the method can be significantly simplified three methods with simpler recording schemes were assessed: (i) a recording scheme that had the same collocation of plateaus but without intermediate plateau (“no-intermediate”); (ii) a staircase scheme from low to high concentrations (“bottom-up”); (iii) a staircase from high to low concentrations (“top-down”). We performed parameter estimations with identical starting values and subsequently compared the complete separation regions as well as the purities obtained from detailed simulations.

Very similar results were obtained for the “no-intermediate” and the “bottom-up” scheme (Fig. 8). In both cases the area of complete separation was lower compared to the area of complete separation obtained with the isotherms derived from the previously validated plateau sequence with intermediate plateaus (see Section 4.3, referred to as “intermediate” in the following) measurement. Interestingly the residual between experimental purities and purities calculated with detailed simulations are comparable to those obtained for the “intermediate” case (Table 5).

However, while the “intermediate” case provides too optimistic results for both raffinate and extract purities (with respect to the graphical treatment, the area of complete separation is slightly too large) parameters obtained using the “bottom-up” and “no-intermediate” approach generally yielded too optimistic purities for the extract and too pessimistic purities for the raffinate (visually speaking the triangle is shifted in direction of the lower left side). The differences in the obtained results are also reflected

**Table 4**  
Comparison of experimental and simulated purities at 25% methanol content.  $E_{\text{exp}}$ : experimental extract purity [%];  $R_{\text{exp}}$ : experimental raffinate purity [%];  $E_{\text{sim}}$ : simulated extract purity [%];  $R_{\text{sim}}$ : simulated raffinate purity [%].

Run	Flow rate ratios				Purity (%)			
	$m_{\text{I}}$	$m_{\text{II}}$	$m_{\text{III}}$	$m_{\text{IV}}$	Experimental		Simulated	
					$E_{\text{exp}}$	$R_{\text{exp}}$	$E_{\text{sim}}$	$R_{\text{sim}}$
M	4.42	1.23	1.51	0.5	> 99	>99	> 99	>99
N	4.47	1.28	1.65	0.65	> 99	93	> 99	90

**Table 5**  
Comparison of experimental purities and simulated purities obtained from different plateau recording schemes—“intermediate”: perturbation method scheme with intermediate plateau; “no-intermediate”: perturbation method scheme without intermediate plateau.  $E_{\text{exp}}$ : experimental extract purity [%];  $R_{\text{exp}}$ : experimental raffinate purity [%];  $E_{\text{sim}}$ : simulated extract purity [%];  $R_{\text{sim}}$ : simulated raffinate purity [%];  $\Delta E = E_{\text{sim}} - E_{\text{exp}}$ ,  $\Delta R = R_{\text{sim}} - R_{\text{exp}}$ .

Run	Purity [%]									
	Experimental		Simulated “intermediate”				Simulated “no-intermediate”			
	$E_{\text{exp}}$	$R_{\text{exp}}$	$E_{\text{sim}}$	$R_{\text{sim}}$	$\Delta E$	$\Delta R$	$E_{\text{sim}}$	$R_{\text{sim}}$	$\Delta E$	$\Delta R$
A	92	100	97	99	5	−1	97	98	5	−2
B	99	100	100	100	1	0	100	99	1	−1
C	100	76	100	80	0	4	100	73	0	−3
D	95	76	98	79	3	3	97	75	2	−1
E	100	100	100	100	0	0	100	100	0	0
F	100	75	100	86	0	11	100	72	0	−3
G	100	100	100	100	0	0	100	97	0	−3
H	100	93	100	100	0	7	100	89	0	−4
I	100	100	100	100	0	0	100	100	0	0
J	95	100	100	100	5	0	100	100	5	0
K	93	100	94	100	1	0	96	100	3	0
L	100	68	100	71	0	3	100	62	0	−6
Sum of $\Delta E$ or $\Delta R$ :					15	26			16	−25

in the deviations in perturbation retention times. In particular, the retention times at smaller concentrations of the “intermediate” approach are significantly higher than the retention times obtained with the “bottom-up” or “no-intermediate” approach, which indicates that the memory effect is less pronounced by these schemes (for a complete list of retention times please refer to Table S5 in the supplementary material). The shifted position of the triangle can mechanistically only be explained by inaccurate isotherm parameterization while the overestimation of the complete separation region is often associated with column

heterogeneity [28,29]. Consequently, the “intermediate” method should be preferred.

When applying the “top-down” scheme very similar results to the “intermediate” case were obtained (Fig. 8) indicating that this method can potentially substitute the experimentally more expensive intermediate plateau approach. In this approach the column is subjected to high concentrations of solute right at the beginning of the procedure for a rather long time leading to an activation of the column. The subsequent plateaus are all approached by desorption from a higher concentration plateau although the difference to the preceding plateau is much reduced compared to the “intermediate” case. Nevertheless the memory-effect seems to be similarly pronounced judging by the retention times at smaller concentrations (Table S5) indicating that the memory effect is captured sufficiently. Consequently, similar good results are obtained in the SMB design.

#### 4.5. Robustness of SMB operation

Long term stability is a crucial property in any continuous process such as an SMB separation. We investigated the robustness of the separation of racemic methionine over a time range of 68 h and chose the operating conditions of experimental point B of Table 2 (10% methanol). After 24 h of stable operation (as judged by constant raffinate and extract purities) the temperature was increased by 1.5 °C and samples were taken to determine the extract and raffinate purities. While the extract purity remained constant at >99% D-methionine, raffinate purity decreased to 98% L-methionine (Fig. 9).

This is in agreement with the general feature of chromatographic separations that adsorption strength and thus retention times decrease with increasing temperature. Decreased adsorption strength leads to lower positions of a putative triangle in the  $m_{\text{II}}-m_{\text{III}}$  plane. Thus, an experimental point that was in the region of complete separation will be in the pure extract (and impure raffinate) region at higher temperature. Preliminary experiments

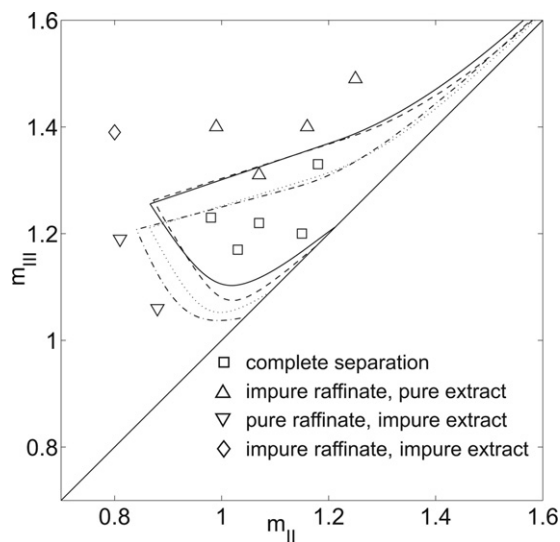


**Fig. 8.** Comparison of complete separation regions obtained from different perturbation method collocation schemes. Solid line: “intermediate”; light dots: “no-intermediate”; dashed: “top-down”; dot-dashed: “bottom-up”.



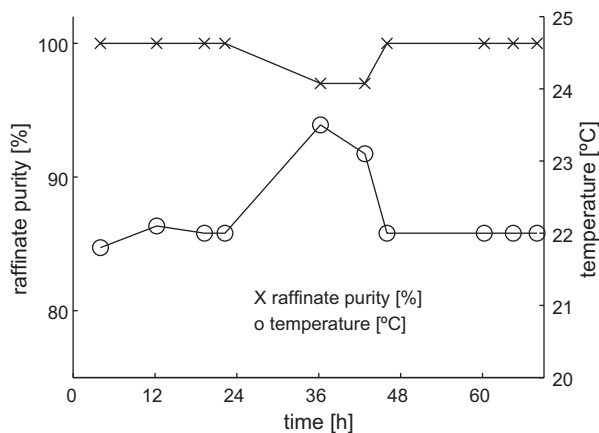


**Fig. 9.** Long term stability of SMB operation. The raffinate purity is strongly dependent on the temperature.

with finite injections at different temperatures already indicated the strong dependence of this chromatographic system on temperature. When operation was returned to the standard 22 °C, raffinate purity again increased to >99% and complete separation, as predicted by simulation, was achieved again. The long term SMB-experiment confirms that the presented chromatographic system is very sensitive towards changes in temperature and therefore requires an adequate temperature control. More importantly, we could demonstrate that stable SMB operation is possible using such memory effect constrained columns supporting our initial assumption that the adsorption behaviour assumes a steady state under SMB conditions.

## 5. Concluding remarks

Stable SMB operation over 3 days clearly suggests that SMB enantioseparation of amino acids employing Chirobiotic TAG columns in aqueous/organic medium constitutes a viable process option despite the well-documented memory effect that severely influences the adsorption behaviour under such conditions. As expected, the key to reliable process design was to ensure an activation of the stationary phase prior to adsorption isotherm determination. To this end, a perturbation method was applied in which the sequence of concentration plateaus was adapted to mimic SMB-like conditions. The obtained parameterizations indeed enabled accurate SMB design as demonstrated by the good agreement between model prediction and experimental SMB runs. This is – to our knowledge – the first report of an SMB enantioseparation of racemic amino acids using commercially available macrocyclic glycopeptide columns. Having demonstrated the usefulness of the design procedure, the true potential of this type of column for amino acid enantioseparation can now be systematically assessed. As we could show in this work the isotherms become more favourable with increasing organic solvent concentration. On the other hand, the solubility of amino acid decreases with increasing methanol-content, thus limiting the feed concentration. Consequently, a true productivity optimum with respect to the organic solvent concentration exists. Obviously identification of

this optimum requires the determination of adsorption isotherms as function of solvent composition, which is well within the scope of the here introduced method.

## Acknowledgements

We acknowledge support from the EU-project “INTENANT”. We thank Shigeharu Katsuo and Prof. Marco Mazzotti for providing the short-cut model and the detailed simulation model, and Prof. Malte Kasperer for help with the perturbation method parameter estimation.

## Appendix A. Supplementary data

Supplementary data associated with this article can be found, in the online version, at doi:10.1016/j.chroma.2012.03.011.

## References

- [1] E. Francotte, *Chirality in Drug Research*, Wiley-VCH Verlag GmbH & Co. KGaA, 2006, p. 155.
- [2] M. Juza, M. Mazzotti, M. Morbidelli, *Trends Biotechnol.* 18 (2000) 108.
- [3] E. Francotte, *J. Chromatogr. A* 906 (2001) 379.
- [4] M. Mazzotti, G. Storti, M. Morbidelli, *J. Chromatogr. A* 769 (1997) 3.
- [5] G. Storti, R. Baciocchi, M. Mazzotti, M. Morbidelli, *Ind. Eng. Chem. Res.* 34 (1995) 288.
- [6] G. Guiochon, A. Felinger, D.G. Shirazi, A.M. Katti, *Fundamentals of Preparative and Nonlinear Chromatography*, 2nd ed., Academic Press, New York, 2006.
- [7] W. Leuchtenberger, K. Huthmacher, K. Drauz, *Appl. Microbiol. Biotechnol.* 69 (2005) 1.
- [8] M.S. Dunn, F.J. Ross, *J. Biol. Chem.* 125 (1938) 309.
- [9] K. Gekko, *J. Biochem.* 90 (1981) 1633.
- [10] C.J. Orella, D.J. Kirwan, *Ind. Eng. Chem. Res.* 30 (1991) 1040.
- [11] D.W. Armstrong, Y. Tang, S. Chen, Y. Zhou, C. Bagwill, J.-R. Chen, *Anal. Chem.* 66 (1994) 1473.
- [12] M. Bechtold, M. Heinemann, S. Panke, *J. Chromatogr. A* 1113 (2006) 167.
- [13] M. Bechtold, A. Felinger, M. Held, S. Panke, *J. Chromatogr. A* 1154 (2007) 277.
- [14] Y.K. Ye, B. Lord, R.W. Stringham, *J. Chromatogr. A* 945 (2002) 139.
- [15] R.W. Stringham, K.G. Lynam, B.S. Lord, *Chirality* 16 (2004) 493.
- [16] J. Putnam, G. Guiochon, *J. Chromatogr. A* 1216 (2009) 8488.
- [17] A. Seidel-Morgenstern, *J. Chromatogr. A* 1037 (2004) 255.
- [18] J. Lindholm, P. Forssén, T. Fornstedt, *Anal. Chem.* 76 (2004) 4856.
- [19] A. Gentilini, C. Migliorini, M. Mazzotti, M. Morbidelli, *J. Chromatogr. A* 805 (1998) 37.
- [20] C. Migliorini, M. Mazzotti, M. Morbidelli, *AIChE J.* 46 (2000) 1384.
- [21] A. Rajendran, G. Paredes, M. Mazzotti, *J. Chromatogr. A* 1216 (2009) 709.
- [22] M. Pedferri, G. Zenoni, M. Mazzotti, M. Morbidelli, *Chem. Eng. Sci.* 54 (1999) 3735.
- [23] S. Abel, M.U. Bähler, C. Arpagaus, M. Mazzotti, J. Stadler, *J. Chromatogr. A* 1043 (2004) 201.
- [24] C. Migliorini, A. Gentilini, M. Mazzotti, M. Morbidelli, *Ind. Eng. Chem. Res.* 38 (1999) 2400.
- [25] C. Heuer, E. Küsters, T. Plattner, A. Seidel-Morgenstern, *J. Chromatogr. A* 827 (1998) 175.
- [26] R. Arnell, P. Forssén, T. Fornstedt, *J. Chromatogr. A* 1099 (2005) 167.
- [27] J.M. Jacobson, J.H. Frenz, C.G. Horvath, *Ind. Eng. Chem. Res.* 26 (1987) 43.
- [28] K. Mihlbachler, J. Fricke, T. Yun, A. Seidel-Morgenstern, H. Schmidt-Traub, G. Guiochon, *J. Chromatogr. A* 908 (2001) 49.
- [29] K. Mihlbachler, A. Jupke, A. Seidel-Morgenstern, H. Schmidt-Traub, G. Guiochon, *J. Chromatogr. A* 944 (2002) 3.
- [30] I. Poplewska, R. Kramarz, W. Piatkowski, A. Seidel-Morgenstern, D. Antos, *J. Chromatogr. A* 1173 (2007) 58.
- [31] P. Jandera, M. Škavřada, K. Klemmová, V. Bačkovská, G. Guiochon, *J. Chromatogr. A* 917 (2001) 123.
- [32] P. Jandera, V. Bačkovská, A. Felinger, *J. Chromatogr. A* 919 (2001) 67.
- [33] R. Arnell, P. Forssén, T. Fornstedt, *Anal. Chem.* 79 (2007) 5838.
- [34] G. Götmar, T. Fornstedt, G. Guiochon, *Chirality* 12 (2000) 558.
- [35] M. Michel, A.A. Epping, Jupke in *Preparative Chromatography*, Wiley-VCH Verlag GmbH & Co. KGaA, 2005, p. 215.